ELSEVIER

1 March 1998

OPTICS COMMUNICATIONS

Optics Communications 148 (1998) 180–186

Full length article

Intensity noise reduction using phase–amplitude coupling in a DFB diode laser

Tiejun Chang, Jean-Philippe Poizat [1], Philippe Grangier

Institut d'Optique, B.P. 147, F-91403 Orsay Cedex, France

Received 21 July 1997; revised 11 November 1997; accepted 12 November 1997

Abstract

We present a detailed investigation of the intensity and phase noise current dependence of a DFB laser diode emitting at 1.3 μm. Phase-amplitude correlations due to the linewidth enhancement factor α are taken into account. The phase to amplitude conversion is realized with a Michelson interferometer. We show that the phase–amplitude correlation is effective only just above threshold and that it goes to zero for increasing current as predicted theoretically by Karlsson and Björk [Phys. Rev. A 44 (1991) 7669]. Our experimental results are well fitted by the standard quantum noise theory of semiconductor lasers providing an additional pumping noise is added. © 1998 Elsevier Science B.V.

PACS: 42.55.Px; 42.50.Dv; 42.62.Fi

1. Introduction

Understanding of the noise of semiconductor lasers has a great importance in fields spanning from optical telecommunications to high-sensitivity spectroscopy. Intensity noise reduction below the shot noise level (SNL) has been demonstrated first by Machida et al. [1] and by many others since then. However the situation is not always very clear when it comes to the comparison between experimental results and theoretical models [2]. For example many types of laser diodes do not exhibit sub-shot noise operation when driven high above threshold as predicted by theory [2]. A first important limitation of these models is that they deal with a single laser mode. It has been pointed out that the presence of weak longitudinal side-modes is of crucial importance for the intensity noise of Fabry-Perot semiconductor lasers [3–6]. Similar mode competition effects have been observed for polarization modes [7]. We think however that further comparison between experiments and theory is needed.

In this work we have used a distributed feedback (DFB) laser with a 40 dB side-mode suppression ratio [8] in order to deal with true single-mode lasers and to avoid the problems arising from side-mode anticorrelations. This diode is driven with a quiet current source. The amplitude and phase noise behavior of this diode is compared with the model of Refs. [2,9] including the linewidth enhancement factor [10]. It appears that the experimental results are well fitted by this model providing an additional Poissonian pumping noise is added.

The laser beam is sent through a Michelson interferometer to investigate both amplitude and phase noise. For a non-zero arm length difference ($l_0 \gg \lambda$) a Michelson interferometer is a dispersive element that rotates the quadrature and that can convert phase noise into amplitude noise when sitting on the side of a fringe. Due to the linewidth enhancement factor (commonly referred to as the α parameter) [10] the phase and amplitude noise are correlated. The minimum noise quadrature is therefore no longer the amplitude. This means that a partial image of the amplitude fluctuations lies in the phase fluctuations, and that by choosing the right linear combination of phase and amplitude quadratures it is possible to find a quadrature whose noise is less than the directly detected amplitude noise

[1] E-mail: jean-philippe.poizat@iota.u-psud.fr

PII S0030-4018(97)00676-7

[11,12]. We have observed experimentally that this correlation decreases as the driving current increases in very good quantitative agreement with the theoretical predictions of Karlsson and Björk [9]. However for a correct description of the intensity noise behavior, a Poissonian pump noise had to be used in the model, although the laser is driven by a noiseless current source. The origin of this excess noise has not yet been identified.

The outline of the paper is the following. The experimental set-up (2.1) and the experimental results (2.2) are presented in Section 2. The theoretical model for the amplitude and phase noise including the effect of the α parameter are detailed in Section 3. Finally in Section 4 the experimental results are compared with the model.

2. Experiment

2.1. Experimental set-up

A sketch of the experimental set-up is shown in Fig. 1. The laser diode is a strained layer multi-quantum well DFB laser [8] emitting at 1.3 μm. Its side-mode suppression ratio is 40 dB [8] and we have checked using the method of Refs. [13,14] that there is no noise contribution coming from eventual longitudinal side-modes. The facet reflection coefficients for the intensity are respectively 0.9 and 0.04. It is driven by a low-noise current source and its temperature is servo-controlled around room temperature. The laser threshold is $I_{th} = 8.8$ mA. Optical isolation of 40 dB is provided by two YIG Faraday rotators and three polarizing cubes.

The light is then sent through a Michelson interferometer with non-zero arm length difference ($l_0 = 0.5$ mm).

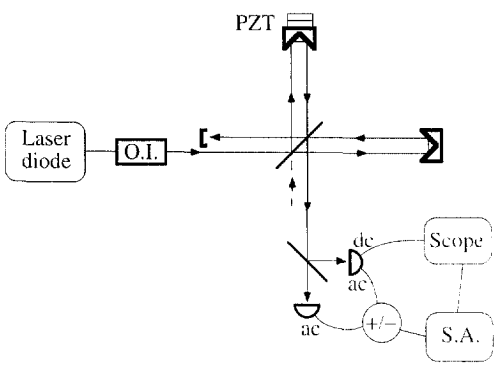

Fig. 1. Experimental set-up. A 30 dB optical isolator avoids spurious feedback in the laser. The path difference is controlled finely by a piezo-electric transducer (PZT) and coarsely by a translation stage (not shown). The ac parts of the photocurrent are either added or subtracted and sent to a spectrum analyser (SA). The dc part of one of the detectors is monitored on an oscilloscope together with the output signal of the SA.

The mirrors of the Michelson interferometer are corner cubes to prevent light from being reflected back into the laser. One of the mirrors is mounted on a piezo-electric transducer (PZT) so that its position can be scanned over the wavelength. The contrast of the interferometer is better than 95%.

The intensity noise of the light coming out of the interferometer is detected in the standard way using a balanced configuration [15]. The SQL is recorded when the power combiner is switched to the − position. The + position gives the total intensity noise. The detectors are high quantum efficiency ($\eta = 0.92 \pm 0.02$) InGaAs photodiodes (Epitaxx ETX 1000). The ac photocurrents are preamplified with a low noise amplifier (OEI model AH0013), combined, and sent to an electronic spectrum analyzer. The noise is analyzed at a frequency $\omega/(2\pi) = 7$ MHz with a 300 kHz resolution bandwidth and a video filter of 30 Hz. The output of the spectrum analyzer is sent to an oscilloscope together with the dc signal of one of the detectors to allow simultaneous recording of the noise and the mean field intensity. The optical transmission of the whole set-up is $T = 62\%$.

2.2. Experimental results

Before presenting the experimental results, let us explain what we mean by quadrature rotation. If we represent the field vector in the complex plane rotating at the optical frequency (cf. Fig. 2), its average value is located on the P axis. The noise appears then as an ellipse where the probability of finding the head of the field vector is more than a given value. When the linewidth enhancement factor α is zero (Fig. 2(a)), the ellipse axes are along the P and Q axis, and their sizes v_p and v_q are the noises of the corresponding quadratures, i.e. $v_p = \sqrt{\langle \delta P^2 \rangle}$ and $v_q = \sqrt{\langle \delta Q^2 \rangle}$. Note that for a semiconductor laser the phase noise which is due to the Schawlow-Townes phase diffusion [16] is much larger than the intensity noise due to the small length of the cavity. If α is now set to a non-zero value (Fig. 2(b)), without changing any other laser parameters, the ellipse becomes longer and thinner and is tilted. According to the formulas derived in Section 3 the amplitude noise is unchanged, and we have $v'_p = v_p$. The phase noise at small RF frequency is enhanced by a factor $1 + \alpha^2$ as already shown by Henry [10] some time ago. The tilt angle θ is given in the limit of large phase noise ($v'_q \gg v'_p$ which is the case for laser diodes) by

$$\theta = C\sqrt{\langle \delta P^2 \rangle / \langle \delta Q^2 \rangle},$$

where C is the normalized correlation between the phase and the amplitude defined below in Eq. (20). Note that this correlation, C, depends of course on α but also on the laser driving current as shown theoretically in Ref. [9]. It is

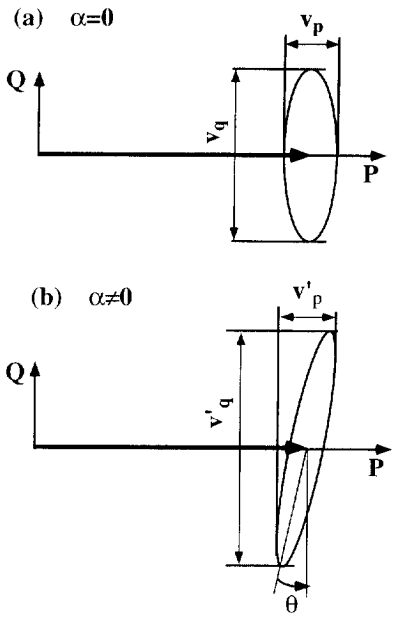

Fig. 2. Representation of the field vector in the rotating complex plane. The ellipse is the contour of equal probability density. In (a) the linewidth enhancement factor is $\alpha = 0$. The small axis of the noise ellipse is on the P axis. The amplitude noise is $\sqrt{\langle \delta P^2 \rangle} = v_p$ and the phase noise is $\sqrt{\langle \delta Q^2 \rangle} = v_q$ In (b) the linewidth enhancement factor is now $\alpha \neq 0$ and all the other laser parameters are identical. The amplitude noise is unchanged and $v'_p = v_p$. The phase noise is enhanced by a factor $1 + \alpha^2$ and is $v'_q = v_q(1 + \alpha^2)$. The noise ellipse is now tilted by an angle $\theta \approx C\sqrt{v'_p / v'_q}$ (when $v'_q \gg v'_p$). Its small axis is no longer on the P axis and its size is $v'_p(1 - C^2)$.

precisely this dependence that we want to check experimentally in this paper.

We have recorded for different values of the driving current the intensity noise at the output of the interferometer while scanning the arm length difference over half the wavelength around a value $l_0 = 0.5$ mm (see Fig. 3).

The shot noise and the intensity noise are recorded together with their corresponding dc current. They are then recombined on the same graph, and the horizontal offset is found by superimposing the dc current traces.

Let us first comment on Fig. 3(b) which is easier to understand since for high values of the driving current the amplitude phase correlation C is almost zero. The double peak structure is due to the conversion on the slopes of a bright fringe of the huge phase noise into amplitude noise. At the very top of a bright fringe, the noise is the amplitude noise of the laser as if it would be directly detected at the output of the laser without the interferometer. If there is no phase–amplitude coupling the noise at the top of a bright fringe corresponds to the minimum noise level. In this case the small axis of the noise ellipse is along the amplitude axis. If there are some correlations between the phase and the amplitude noise, the minimum noise is no longer at the top of a bright fringe, and the noise trace becomes asymmetric. This occurs because in this situation the noise ellipse is tilted and its small axis is no longer the amplitude axis. This asymmetric behaviour is weak but present in Fig. 3(b), showing a small but non-zero amplitude phase correlation C ($|C| = 0.15$).

In Fig. 3(a), the laser is driven just above threshold ($I/I_{th} = 1.4$). The noise trace displays a very asymmetric profile, and the minimum noise is obtained clearly on the side of the bright fringe. This is the signature of a rather strong phase–amplitude coupling and the fitting gives indeed a normalized correlation $|C| = 0.75$.

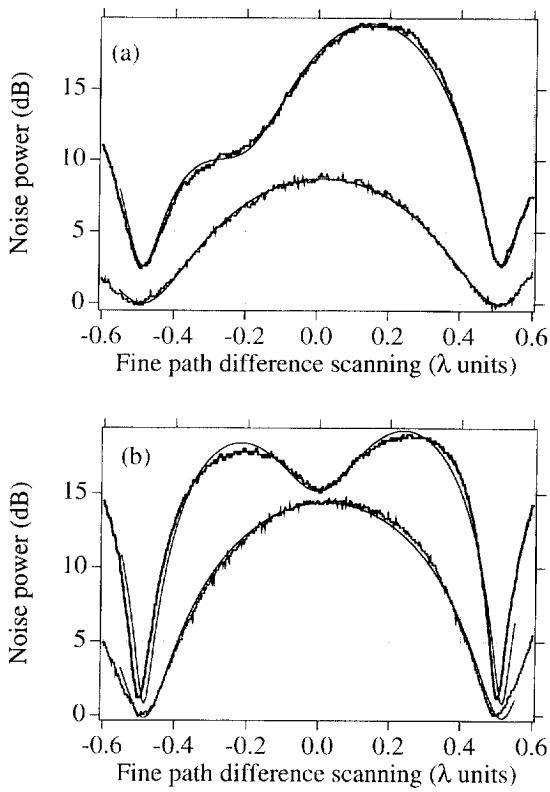

Fig. 3. Example of fine PZT scans. Raw experimental results (thick line) and best fitting (thin line) using Eq. (A.3) of Appendix A, where the electronic noise has been added. The bottom trace is the SNL, and the upper trace is the intensity noise at the output of the interferometer. The scanning time is about 1 s, the resolution bandwidth is 300 kHz and the video bandwidth is 30 Hz. For graph (a) the driving current is $I = 11$ mA, and the fitting parameters are $\langle \delta P^2 \rangle = 14.3$, $\langle \delta Q^2 \rangle = 1.2 \times 10^9$, $C = -0.75$. For graph (b) $I = 60$ mA and the fitting gives $\langle \delta P^2 \rangle = 1.2$, $\langle \delta Q^2 \rangle = 8 \times 10^8$, and $C = -0.15$.

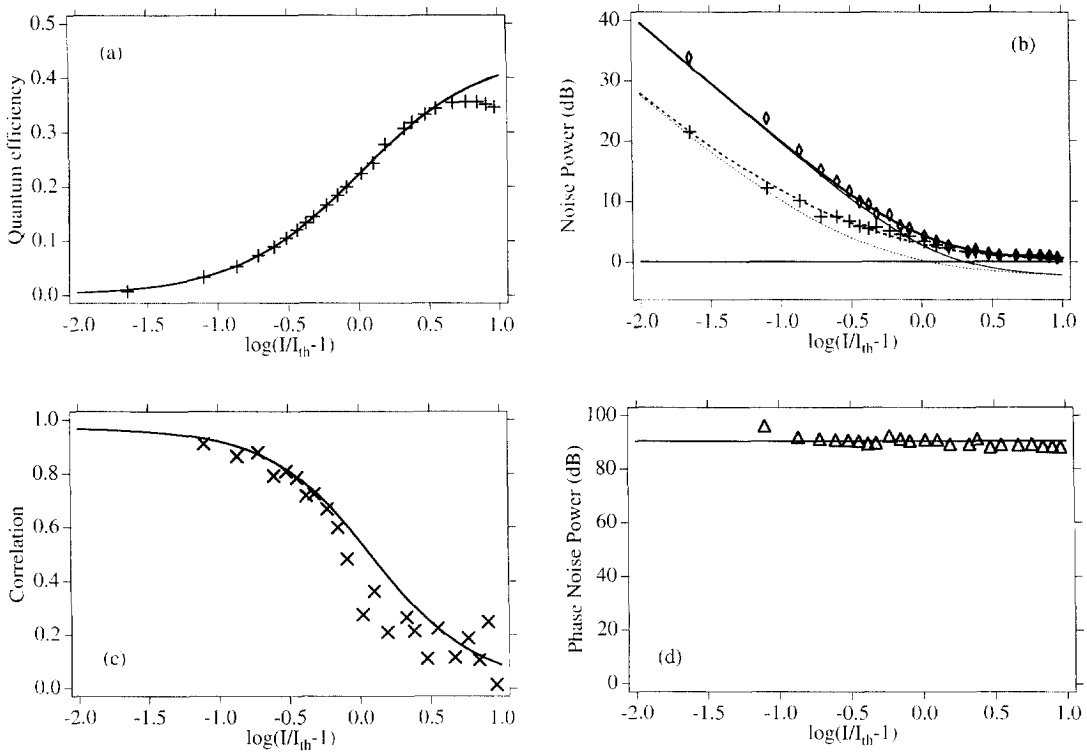

Fig. 4. (a) quantum efficiency versus the normalized driving current. In all the following graphs the noise has been detected at $\omega/(2\pi) = 7$ MHz. (b) Uncorrected and corrected intensity noise. The ($\diamond$) symbols fitted by the thick solid line correspond to the intensity noise detected at the top of a bright fringe versus the normalized driving current I/I_{th}. The (+) symbols fitted by the thick dashed line correspond to the minimum noise. It corresponds to the intensity noise corrected by the correlated phase noise. The thin solid and dashed lines are the theoretical predictions for a noiseless pump respectively for the uncorrected and the corrected intensity noise. The 0 dB level corresponds to the SNL. (c) Normalized correlations $|C|$ (note that the first experimental point has been removed because of the difficulty of obtaining an accurate value from the experimental data). (d) Phase noise. The 0 dB level corresponds to the SNL. The parameters for the fittings are the same for the 4 graphs and are: $\tau_{sp} = 10^{-9}$ s, $\tau_{pe} = 6 \times 10^{-12}$ s, $\tau_{po} = 0.8\tau_{pe}$, $\alpha = 4$, $\epsilon = 1$, $I_{th} = 8.8$ mA, $\omega/(2\pi) = 7$ MHz. The data presented in these graphs have been corrected for the electronic noise and for the optical transmission of the set-up ($T = 0.62$) and quantum efficiency of the detectors ($\eta = 0.92$).

The experimental traces have been fitted by the expression given in Appendix A, with the intensity noise the phase noise and their correlation as adjustable parameters. So this allow us to infer the magnitude of these three parameters which are given in the caption of Fig. 3.

Similar graphs were recorded for 24 values of the driving current ranging from $I/I_{th} = 1.02$ to $I/I_{th} = 10.2$. For each of these graphs the noise at the top of a bright fringe and the minimum noise have been measured experimentally and have been displayed versus $\log(I/I_{th})$ in Fig. 4(b). Each of these 24 graphs has been fitted as in Fig. 3, and the corresponding parameters $\langle \delta P^2 \rangle$, $\langle \delta Q^2 \rangle$, and $C = \langle \delta P \delta Q \rangle$ have been extracted. It can be noted that the value of the intensity noise coming from the fitting corresponds to the value directly measured on the experimental trace to better than 1 dB. The normalized correlation coefficient C and the phase noise obtained from the fittings have been plotted versus I/I_{th} in Fig. 4(c) and 4(d) respectively.

The graphs of Fig. 4(b), 4(c) show clearly that the phase–amplitude noise correlations decrease as the driving current increases as predicted in Ref. [9]. Moreover, these experimental results are very well fitted by a theoretical model similar to the one of Refs. [2,9]. A detailed derivation of this model is presented in Section 3. And the comparison between experiments and theory will then be made and discussed in Section 4.

3. Theoretical model

In this section, we present in detail a theoretical model of a single mode laser diode including phase noise effects. This model is based on coupled Langevin type equations for the evolution of the electro-magnetical field $a(t)$ of the laser and the evolution of the excited carrier population $N(t)$ [2,9]. It is identical to the model used in Ref. [9], but

has been simplified for our purpose. The electro-magnetic field is considered here as a complex number and we have

$$\frac{da(t)}{dt} = \left[-\frac{1}{2}\left(\frac{1}{\tau_{pe}} + \frac{1}{\tau_{po}} + 2i\Delta \right) + \frac{N(t)A}{2}(1 - i\alpha) \right] a(t) + \left(\gamma_r^{(pe)}(t) + i\gamma_i^{(pe)}(t) \right) + \left(\gamma_r^{(po)}(t) + i\gamma_i^{(po)}(t) \right) + \left(\xi_r(t) + i\xi_i(t) \right), \tag{1}$$

where $1/\tau_{pe}$ is the photon decay rate due to the coupling mirror, $1/\tau_{po}$ is the photon decay rate due to intracavity optical losses. The coefficient A is the spontaneous emission rate of the lasing mode. The detuning Δ is such that the mean value of the imaginary part of the rhs of Eq. (1) is zero, and fulfils therefore the condition $\Delta = -\alpha A\langle N(t)\rangle/2$ that defines the frequency of the laser. The α parameter is the phase–amplitude coupling coefficient [10]. The last terms are Langevin noise terms decomposed into their real and imaginary parts. All these Langevin function are real numbers. The mean field is chosen as real and gives the phase reference. The $\gamma^{(pe)}(t)$ terms are associated with the output coupling. Their non-zero correlations are

$$\langle \gamma_i^{(pe)}(t)\gamma_i^{(pe)}(t')\rangle = \langle \gamma_r^{(pe)}(t)\gamma_r^{(pe)}(t')\rangle = \delta(t-t')/4\tau_{pe}. \tag{2}$$

The $\gamma^{(po)}(t)$ terms correspond to the intracavity losses. Their non-zero correlations are given by

$$\langle \gamma_i^{(po)}(t)\gamma_i^{(po)}(t')\rangle = \langle \gamma_r^{(po)}(t)\gamma_r^{(po)}(t')\rangle = \delta(t-t')/4\tau_{po}. \tag{3}$$

Finally the $\xi(t)$ terms concern the noise associated with the stimulated emission. Their non-zero correlations are

$$\langle \xi_r(t)\xi_r(t')\rangle = \langle \xi_i(t)\xi_i(t')\rangle = \delta(t-t')A\langle N\rangle/4. \tag{4}$$

The equation of motion for the total excited carrier number $N(t)$ is

$$\frac{dN(t)}{dt} = P - \frac{N(t)}{\tau_{sp}} - A(n(t)+1)N(t) + \Gamma^{(p)}(t) + \Gamma^{(sp)}(t) + \Gamma(t), \tag{5}$$

where P is the pumping rate, τ_{sp} is the spontaneous electron lifetime, and $n = a^{\dagger}a$ is the photon number in the cavity mode. The last three terms are Langevin noises. The first one $\Gamma^{(p)}(t)$ is associated with the pump noise, its correlation function is

$$\langle \Gamma^{(p)}(t)\Gamma^{(p)}(t')\rangle = \delta(t-t')\epsilon P, \tag{6}$$

where $\epsilon = 0$ for a pump noise suppressed laser, and $\epsilon = 1$ for a laser driven by a Poissonian pump. The second and third one $\Gamma^{(sp)}(t)$ and $\Gamma(t)$ are respectively associated with spontaneous and stimulated emission noise. Their non-zero correlations are

$$\langle \Gamma^{(sp)}(t)\Gamma^{(sp)}(t')\rangle = \delta(t-t')\langle N\rangle/\tau_{sp}, \tag{7}$$

$$\langle \Gamma(t)\Gamma(t')\rangle = \delta(t-t')A\langle N\rangle\langle n\rangle. \tag{8}$$

Finally, due to their same physical origin, the noise terms associated with the stimulated gain for the photons and stimulated-emission for the electrons are perfectly anticorrelated and have cross-correlations

$$\langle \Gamma(t)\xi_r(t')\rangle = -\delta(t-t')A\langle N\rangle\sqrt{\langle n\rangle/4}. \tag{9}$$

Note that all the other correlations and cross-correlations are zero.

The stationary solutions for the internal photon number $\langle n\rangle$ when the laser is lasing (i.e. $n \gg 1$) have simple analytical expressions

$$\langle n\rangle = P\tau - 1/A\tau_{sp}, \tag{10}$$

$$\langle N\rangle = 1/A\tau, \tag{11}$$

with $1/\tau = 1/\tau_{pe} + 1/\tau_{po}$. Note that in the following, all the analytical formulas will be obtained within the approximation $n \gg 1$.

Let us now define respectively the field amplitude quadrature P and the phase quadrature Q by

$$P = (a + a^{\dagger})/2, \tag{12}$$

$$Q = (a - a^{\dagger})/(2i). \tag{13}$$

Expressions for the internal amplitude fluctuations δP and phase fluctuations δQ are obtained from the linearization of Eqs. (1) and (5). The corresponding output fluctuations are obtained using the usual input–output relations,

$$P_{out} = \frac{1}{\sqrt{\tau_{pe}}} P - \sqrt{\tau_{pe}}\,\gamma_r, \tag{14}$$

$$Q_{out} = \frac{1}{\sqrt{\tau_{pe}}} Q - \sqrt{\tau_{pe}}\,\gamma_i. \tag{15}$$

Note that in these relations quantities without the *out* subscript are internal quantities.

It is then straightforward to obtain the variance of the zero-frequency output amplitude fluctuations using the

above formulas and the Langevin noise correlations given above (Eqs. (2)–(9)). It gives

$$\langle \delta P_{\text{out}}^2 \rangle = \left(\frac{\tau\left(1/\tau_{\text{sp}} + A\langle n\rangle\right)}{2\sqrt{\tau_{\text{pc}}}\, A\langle n\rangle} - \frac{\sqrt{\tau_{\text{pc}}}}{2} \right)^2 \frac{1}{\tau_{\text{pc}}} + \left(\frac{\tau\left(1/\tau_{\text{sp}} + A\langle n\rangle\right)}{2\sqrt{\tau_{\text{pc}}}\, A\langle n\rangle} \right)^2 \left(\frac{2}{\tau} - \frac{1}{\tau_{\text{pc}}} \right) + \frac{(\epsilon - 1)\tau\left(1/\tau_{\text{sp}} + A\langle n\rangle\right)}{4\tau_{\text{pc}} A\langle n\rangle}. \tag{16}$$

Note that the zero-frequency expression is valid for RF frequency such that $\omega \ll 1/\tau_{\text{sp}}$.

The phase noise $\langle \delta Q_{\text{out}}^2 \rangle$ at a low RF frequency $\omega/(2\pi)$ (i.e. $\omega \ll 1/\tau_{\text{sp}}$) is given by

$$\langle \delta Q_{\text{out}}^2 \rangle = \frac{1}{2\tau_{\text{pc}}} \left(\frac{1+\alpha^2}{\tau\omega^2} + \frac{\tau_{\text{pc}}}{2} \right). \tag{17}$$

It can be observed that for low frequencies the last term can be neglected and the frequency noise is then the standard Schawlow-Townes phase noise [16] broadened by the factor $1 + \alpha^2$ as demonstrated by Henry [10].

We calculate now the symmetrized correlation between the output frequency and amplitude fluctuations. We obtain

$$\langle \delta Q_{\text{out}} \delta P_{\text{out}} \rangle = \frac{\alpha}{2\tau_{\text{pc}}\tau_{\text{sp}} A\langle n\rangle \omega}. \tag{18}$$

It is important to notice that the correlation is proportional to the phase–amplitude coupling coefficient α as expected. It is also proportional to $1/\langle n\rangle$ and goes to zero for increasing $\langle n\rangle$.

The minimum noise taking advantage of the correction due to the phase–amplitude coupling is [9]

$$\langle \delta P_{\text{cor}}^2 \rangle = \langle \delta P_{\text{out}}^2 \rangle (1 - C^2), \tag{19}$$

where C is the normalized correlation given by

$$C = \frac{\langle \delta Q_{\text{out}} \delta P_{\text{out}} \rangle}{\sqrt{\langle \delta Q_{\text{out}}^2 \rangle \langle \delta P_{\text{out}}^2 \rangle}}. \tag{20}$$

The analytical formula for C cannot be easily simplified. It can however easily be shown that its maximum is $\alpha/\sqrt{1+\alpha^2}$ for vanishing photon number $\langle n\rangle$. Note that this corrected noise, $\langle \delta P_{\text{cor}}^2 \rangle$, corresponds to the size of the small axis of the ellipse (cf. Fig. 2) and to the minimum noise level in Fig. 3.

4. Discussion

The total quantum efficiency, defined as the number of photons coming out of the laser divided by the number of electrons going through the laser, has been plotted versus the normalized driving current in Fig. 4(a). This parameter characterizes the mean value behavior of the laser. The agreement with theory is perfect for a driving current smaller than 50 mA. For currents higher than that value thermal effects decrease the efficiency of the laser.

In Fig. 4(b) the intensity noise at the top of a bright fringe, and the minimum noise (cf. Fig. 3) with respect to the driving current are plotted. These values are corrected for the transmission efficiency $T = 0.62$ and for the photodiodes quantum efficiency $\eta = 0.92$. The intensity noise at the top of a bright fringe is the intensity noise that would be detected directly on a photodiode without the interferometer. The minimum noise is the intensity noise corrected by its correlation with the phase noise. It can be seen that neither the directly detected intensity noise nor the corrected noise go below the SNL. But the theoretical predictions prescribe that for a noiseless pump the uncorrected and corrected noise should be below the SNL when the driving current is respectively larger than 25 mA and 20 mA. We had then to artificially add a Poissonian pump noise to model properly our experimental results. We have of course checked that this excess noise is not coming from the laser power supply. The real physical origin of this noise source is not clear and is far beyond the scope of this paper. Let us mention that the production of squeezed light from some laser diodes has already unambiguously been observed (see for example Ref. [17]) according to the theory of Ref. [2]. Note that the fact that the experimental data can not be fitted by a noiseless pump is not due to thermal effects, which take place only for large driving currents ($I > 50$ mA).

Fig. 4(c) and 4(d) respectively display the normalized correlation $|C|$ and the phase noise (relative to the SNL) deduced from the fittings of 24 fine scan graphs as those in Fig. 3. The constant phase noise corresponds to the Schawlow-Townes phase diffusion noise. As previously these quantities are corrected for the transmission efficiency $T = 0.62$ and for the photodiode quantum efficiency $\eta = 0.92$. It should be noted that the values obtained from the first graph (i.e. for $I = 9$ mA) have been discarded due to the poor sensitivity of the fitting to the values of the correlation and the phase noise.

For the correlation, the agreement with theory is very good. It reaches its maximum value $\alpha/(1+\alpha^2)$ just above threshold, and goes to zero for large driving currents. The value of the linewidth enhancement factor α given by the fittings is $\alpha = 4 \pm 1$.

According to the theory the phase noise should not depend on the driving current. The relatively large dispersion on the experimental values is due to the fact that the arm length difference is chosen so that the correlation effects are clearly visualized but is too small to allow precise estimation of the phase.

It has to be emphasized that all the fittings of Fig. 4 have been performed with the same set of parameters. The

agreement with theory, for the mean values as well as for the noises, is very good. The driving current dependence of the noise reduction due to the phase–amplitude coupling is well reproduced. However the data presented in this paper show quantitatively that some devices suffer from an excess noise which is not included in the simple model of Ref. [2], and which was here added in a phenomenological way as a Poissonian pumping noise.

5. Conclusion

The purpose of this paper was to present a detailed comparison between the experimental amplitude and phase quantum noise behavior (including the α parameter) of a DFB semiconductor laser and the standard theory of Refs. [2,9]. We have clearly observed the noise reduction associated with phase–amplitude coupling for low driving currents [9]. The agreement with theory is excellent providing we phenomenologically add a Poissonian pump noise to describe the fact that the intensity noise never goes below the SNL for large driving currents. We have not yet identified the physical origin of this excess noise. Possible hints could perhaps be found in Refs. [18,19]. In these papers, the effects on noise of the spatial distribution of the field intensity along the cavity are considered (see also Ref. [20]). We are currently investigating these problems more quantitatively in the situations corresponding to our lasers.

Acknowledgements

We thank B. Fernier from Alcatel-Alsthom for providing us the DFB laser. T.J.C. is Boursier du Gouvernement Français. This work was supported by the ESPRIT European Long Term Research program (ACQUIRE 20029) and by the Ultimatech CNRS program.

Appendix A. Quadrature rotation after propagation in a Michelson interferometer

In this appendix, we give the formula for the intensity noise after rotation of the quadratures due to the propagation of a laser beam in a Michelson interferometer. An explicit derivation of this formula is given in Appendix A of Ref. [14].

Let us first define the following parameters

$$\mathscr{A} = \cos(k(l_0 + x)), \quad \mathscr{B} = \sin(k(l_0 + x)),$$
$$\mathscr{C} = \cos(\omega l_0/c), \quad \mathscr{D} = \sin(\omega l_0/c), \tag{A.1}$$

where $k = 2\pi/\lambda$ (λ is the light wavelength), $l_0 + x$ is the interferometer arm length difference, where $x \in [-\lambda/2, \lambda/2]$ is the fine scan of the mirror position around l_0. The quantity $\omega/(2\pi)$ is the RF noise analysis frequency.

The shot noise level $S(x)$ is given by

$$S(x) = (1 - Q)/(1 + Q) + Q\mathscr{A}^2, \tag{A.2}$$

where Q is the fringe contrast.

The intensity noise level $N(x)$ at the output of the interferometer can then be written as

$$\begin{aligned} N(x) = S(x)\Big\{ & \mathscr{A}\mathscr{C}\left[\mathscr{A}\mathscr{C}\langle \delta P^2\rangle - \mathscr{B}\mathscr{D}\langle \delta P \delta Q\rangle\right] \\ & - \mathscr{B}\mathscr{D}\left[\mathscr{A}\mathscr{C}\langle \delta P \delta Q\rangle - \mathscr{B}\mathscr{D}\langle \delta Q^2\rangle\right] \\ & + \left[\mathscr{A}\mathscr{D}\right]^2 + \left[\mathscr{B}\mathscr{C}\right]^2\Big\}, \end{aligned} \tag{A.3}$$

where $\langle \delta P^2\rangle$, $\langle \delta Q^2\rangle$, $\langle \delta P \delta Q\rangle$ are respectively the amplitude noise, phase noise, and their symmetrized correlation, at the output of the laser (i.e. the input of the interferometer) as defined in Section 3. Note that the out subscript has been omitted for clarity. Eq. (A.3), where a constant term has been added to describe the electronic noise, is the formula used in the fittings of Fig. 3. These last three parameters are the adjustable parameters used in these fittings. The intensity and phase noise are given relatively to the SNL, i.e. a value of 1 is the SNL.

References

[1] S. Machida, Y. Yamamoto, Y. Itaya, Phys. Rev. Lett. 58 (1987) 1000.
[2] Y. Yamamoto, S. Machida, O. Nilsson, Phys. Rev. A 34 (1986) 4025.
[3] A.W. Smith, J.A. Armstrong, IBM J. 10 (1966) 225.
[4] H. Wang, M.J. Freeman, D.G. Steel, Phys. Rev. Lett. 71 (1993) 3951.
[5] J. Kitching, A. Yariv, Y. Shevy, Phys. Rev. Lett. 74 (1995) 3372.
[6] F. Marin, A. Bramati, E. Giacobino, T.-C. Zhang, J.-Ph. Poizat, J.-F. Roch, P. Grangier, Phys. Rev. Lett. 75 (1995) 4606.
[7] D.C. Kilper, D.G. Steel, R. Craig, D.R. Scifres, Optics Lett. 21 (1996) 1283.
[8] B. Fernier, F. Gerard, P. Pagnod, G. Michaud, G. Ripoche, G. Vendrome, R.M. Capella, Electron. Lett. 31 (1995) 2174.
[9] A. Karlsson, G. Björk, Phys. Rev. A 44 (1991) 7669.
[10] C.H. Henry, IEEE J. Quantum Electron. 18 (1982) 259.
[11] M.A. Newkirk, K.J. Vahala, IEEE J. Quantum Electron. 27 (1991) 13.
[12] K. Kikuchi, K. Watanabe, K. Katoh, Appl. Phys. Lett. 65 (1994) 2533.
[13] S. Inoue, Y. Yamamoto, Optics Lett. 22 (1997) 328.
[14] J.Ph. Poizat, P. Grangier, J. Opt. Soc. Am. B 14 (1997) 2772.
[15] H.P. Yuen, V.W.S. Chan, Optics Lett. 8 (1983) 177.
[16] A.L. Schawlow, C.H. Townes, Phys. Rev. 112 (1958) 1940.
[17] S. Machida, Y. Yamamoto, Phys. Rev. Lett. 60 (1988) 792.
[18] B. Tromborg, H.E. Lassen, H. Olesen, IEEE J. Quantum Electron. 30 (1994) 939.
[19] D.D. Marcenac, J.E. Carroll, IEEE J. Quantum Electron. 30 (1994) 2064.
[20] M. Yamashita, S. Machida, T. Mukai, O. Nillson, Optics Lett. 22 (1997) 534.